Iterative Beamspace Covariance Refinement for Precise DOA Estimation in Uniform Circular Arrays under Low-snapshot Conditions

Mahdi Sharifi

Semnan University, Semnan, Iran

https://doi.org/10.26636/jtit.2026.1.2392

Abstract — Uniform circular arrays (UCA) provide 360° angular coverage and uniform directional response, making them preferable for direction-of-arrival estimation (DOAE). This paper proposes an iterative enhancement technique for root-MUSIC-based methods under UCA configurations, particularly effective in low-snapshot scenarios. The idea is to iteratively refine the beamspace sample covariance matrix (BSCM) by estimating and suppressing residual components that alter the signal and noise subspaces. This refinement significantly improves the accuracy of DOAE, even under limited data conditions. Numerical simulations demonstrate that the proposed method outperforms conventional UCARM, sparse UCARM, UCARBRM and unitary UCARM algorithms in terms of estimation error, beamspace leakage, conditional mean square error (CMSE) and resolution probability – across uncorrelated and correlated signal scenarios. The proposed technique is also applicable to RARE-based approaches for 2D DOAE, while preserving the beamspace covariance structure. Furthermore, the proposed method is suitable for electronic surveillance systems and low-power sensor networks.

Keywords — beamspace covariance matrix, direction of arrival estimation, low snapshot, root-MUSIC, subspace leakage, uniform circular array

1. Introduction

Uniform circular arrays (UCA) [1] provide 360° azimuthal coverage with consistent directional characteristics across elevation angles, making them a strong candidate for electronic intelligence and direction-finding applications [2]–[10]. To improve the accuracy of direction-of-arrival estimation (DOAE), the beamspace transform (BT) technique – typically applied in phase mode – is used in UCAs. This transform not only ensures low estimation error, but also enables high-resolution processing with reduced computational complexity.

Several BT-based DOAE algorithms have been developed, including real beamspace root-MUSIC (UCARBRM), UCA-ESPRIT, and spatial smoothing techniques for correlated signal scenarios. The UCA-ESPRIT algorithm was presented in [11], while methods to address correlated signals have been explored in [12]–[15]. Root-MUSIC (RM), which avoids spectral search through polynomial rooting, was originally proposed for uniform linear arrays (ULA) [16] and has since been widely extended and applied [17], [18]. With the application of BT, RM was adapted to UCAs for azimuth estimation. In [19]–[21], the unitary version of UCA-RM (UCARM) demonstrated strong performance in correlated and uncorrelated environments. For sparse UCA configurations, sparse UCARM was proposed in [22], [23], although it lacks centro-Hermitian symmetry in the beamspace manifold.

To reduce the estimation bias introduced by standard BT, a modified beamspace transform (MBT) was introduced in [24]. Furthermore, pseudo noise resampling methods were studied in [21], [25] to mitigate the influence of outliers, although these approaches typically rely on a large number of snapshots for accurate estimation.

In [26], a two-sided correlation transformation (TCT) approach was proposed, leveraging array manifold interpolation (AMI) to reconstruct the signal covariance matrix under low signal-to-noise ratio (SNR) conditions. Similarly, a two-step RM method introduced in [27] aimed to improve the performance of DOAE under limited snapshot availability. Root-SWAP RM, based on a stochastic maximum likelihood criterion, was also proposed for ULA-based azimuth-only estimation scenarios.

Despite these advances, most existing approaches focus primarily on modified transforms, resampling strategies, or reconstruction techniques, while the direct refinement of the beamspace sample covariance matrix (BSCM) itself in limited-snapshot regimes has received comparatively less attention. Moreover, classical subspace perturbation analyses provide general insight into estimation errors, but they do not explicitly address structured residual components arising in the beamspace domain.

This paper proposes an iterative refinement technique for computationally efficient DOAE using UCAs in limited-snapshot regimes. The approach is applicable to both 1D and 2D frameworks, such as RM and RARE. Using UCARM as a representative example, the method begins by applying BT to convert element-space data into beamspace, followed by initial DOA estimation via RM. The BSCM is then iteratively refined

to remove residual components, producing more accurate and unbiased DOA estimates.

The remainder of this paper is organized as follows. Section 2 presents a model of the system; Section 3 introduces the proposed method. Performance analysis is presented in Section 4, while Section 5 discusses simulation results. Section 6 concludes the paper.

2. Signal Modeling

Assume that a UCA with radius R consists of P omnidirectional antenna elements. K is considered to be the narrowband signals from the far field impinging on the antenna array with the directions $(\theta_k, \varphi_k), k = 1, 2, \ldots, K$, where $\theta_k \in [0, \frac{\pi}{2}]$ and $\varphi_k \in [0, 2\pi]$ denote the elevation and azimuth angles of the k-th signal, respectively. Suppose that N snapshots are observed by the array. The measurements of the $P \times N$ array can be considered as:

$$\mathbf{X} = \big[x(1), \ldots, x(N)\big] = \mathbf{A}\,\mathbf{S} + N\,, \tag{1}$$

where $\mathbf{A} \in \mathbf{C}^{P\times K}$ is the element space manifold, $\mathbf{S} = [s(1), \ldots, s(N)] \in \mathbf{C}^{K\times N}$ is the signal, and $\mathbf{N} \in \mathbf{C}^{P\times N}$ is the white Gaussian noise.

Here, signal and noise are uncorrelated. The element space manifold $\mathbf{A}$ is given by:

$$\mathbf{A} = \big[\boldsymbol{a}(\theta_1, \varphi_1), \boldsymbol{a}(\theta_2, \varphi_2), \ldots, \boldsymbol{a}(\theta_K, \varphi_K)\big]\,, \tag{2}$$

where

$$\boldsymbol{a}(\theta_1, \varphi_1) = \big[e^{ikR\sin(\theta_i)\cos(\varphi_i - r_1)}, e^{ikR\sin(\theta_i)\cos(\varphi_i - r_2)}, \ldots, e^{ikR\sin(\theta_i)\cos(\varphi_i - r_p)}\big]^T\,. \tag{3}$$

In the above equation $r_p = \frac{2\pi p}{P}, p = 0, 1, \ldots, P-1$ is the element location, $k = \frac{2\pi}{\lambda}$ is the wavenumber, λ is the wavelength, and $[\cdot]^T$ is the transpose operation.

In [25], the beamforming matrix $\mathbf{W}$ was utilized for the transformation from element space manifold to beamspace manifold and $\mathbf{W}$ is given by:

$$\mathbf{W} = \sqrt{P}\big[\boldsymbol{w}_{-M}, \ldots, \boldsymbol{w}_0, \ldots, \boldsymbol{w}_M\big]\,, \tag{4}$$

where $\boldsymbol{w}_m^H = \frac{1}{P}\big[e^{imr_1}, \ldots, e^{imr_p}\big]$ with $(\cdot)^H$ is considered as the factor of weight which is denoting the Hermite transformation.

Similarly, $M = [kR]$ with $[\cdot]$ is considered as the highest order mode at the ceiling operation. Then the $(2M+1) \times K$ beamspace manifold is given as:

$$\mathbf{B} = \big[b(\theta_1, \varphi_1), \ldots, b(\theta_K, \varphi_K)\big] = \mathbf{W}^H\mathbf{A}\,, \tag{5}$$

where:

$$\boldsymbol{b}(\theta_i, \varphi_i) = \mathbf{W}^H\boldsymbol{a}(\theta_i, \varphi_i) \approx \mathbf{F}(\theta_i)\,\boldsymbol{a}_e(\varphi_i)\,. \tag{6}$$

$\mathbf{F}(\theta_i) = \mathrm{diag}[a_{-M}(\theta_i), \ldots, a_M(\theta_i)]$ and $a_M(\theta_i) = j^m J_m(kR\,\sin\theta_i)$ with J_m is the first kind of Bessel function for the order m and $a_e(\varphi_i) = [e^{-jM\varphi_i}, \ldots, e^0, \ldots, e^{jM\varphi_i}]^T$.

According to Eqs. (1) and (5), the beamspace data have the following form:

$$\mathbf{Y} = \big[\boldsymbol{y}(1), \ldots, \boldsymbol{y}(N)\big] = \mathbf{W}^H(\mathbf{AS} + \mathbf{N}) = \mathbf{W}^H\mathbf{AS} + \mathbf{N}_1\,, \tag{7}$$

where $\mathbf{N}_1 = \mathbf{W}^H\mathbf{N}$ as the white Gaussian noise of the beamspace via distribution is $(0, \sigma_1^2 I_{2M+1}) \cdot I_{2M+1}$ and σ_1^2 are the matrix of identity and the beamspace noise power, respectively. Considering the system model from Eq. (7), the $(2M+1) \times (2M+1)$ beamspace true covariance matrix is expressed as:

$$\begin{aligned}\mathbf{R}_y &= E\left\{\boldsymbol{y}(n), \ldots, \boldsymbol{y}^H(n)\right\} \\ &= \mathbf{W}^H\mathbf{A}\mathbf{R}_s\mathbf{A}^H\mathbf{W} + \sigma_1^2\,\mathbf{I}_{2M+1}\end{aligned}\,, \tag{8}$$

where $\mathbf{R}_s = E\{\boldsymbol{s}(n)\boldsymbol{s}^H(n)\} \in \mathbf{C}^{K\times K}$ and $E\{\cdot\}$ represent and denote the covariance matrix of true signal and the expectation operator, respectively.

Perform the beamspace's eigenvalue-decomposition (EVD) true matrix of covariance, and let $\{\lambda_1, \ldots, \lambda_K, \lambda_{K+1}, \ldots, \lambda_{2M+1}\}$ which are arranged in a non-increasing order be the beamspace true eigenvalues corresponding to beamspace true eigenvectors $\{e_1, \ldots, e_K, \ldots, e_{2M+1}\}$. Then, we have the beamspace true signal subspace $\mathbf{E}_s = \{e_{K+1}, e_{K+2}, \ldots, e_{2M+1}\}$ and the noise subspace $\mathbf{E}_n = \{e_{K+1}, e_{K+2}, \ldots, e_{2M+1}\}$.

3. Proposed Technique

To illustrate the proposed technique, we utilize the UCARM method for azimuth angle estimation as an example. Suppose the elevation angle is fixed, then the beamspace manifold can be considered as a Vandermonde matrix when the number of antenna elements is large enough, and the UCARM root polynomial of UCARM is:

$$f(\varphi) = \boldsymbol{a}_e^H(\varphi)\,\mathbf{F}^H(\theta)\,\mathbf{E}_n\,\mathbf{E}_n^H\,F(\theta)\,\boldsymbol{a}_e(\varphi)\,. \tag{9}$$

The DOAs can be obtained from the K largest roots of the polynomial formulated in Eq. (9) located inside the unit circle. According to the mathematical formula, the BSCM can be rewritten as [27]:

$$\begin{aligned}\hat{R}_y =& \frac{1}{N}\sum_{n=1}^{N}\left(\mathbf{W}^H\mathbf{A}\boldsymbol{s}(n) + \boldsymbol{n}_1(n)\right)\left(\mathbf{W}^H\mathbf{A}\boldsymbol{s}(n) + \boldsymbol{n}_1(n)\right)^H \\ &= \mathbf{W}^H\mathbf{A}\mathbf{R}_s\mathbf{A}^H\mathbf{W} + \sigma_1^2\,\mathbf{I}_{2M+1} \\ &+ \mathbf{W}^H\mathbf{A}\left\{\frac{1}{N}\sum_{n=1}^{N}\boldsymbol{s}(n)\boldsymbol{n}_1^H(n)\right\} \\ &+ \left\{\frac{1}{N}\sum_{n=1}^{N}\boldsymbol{n}_1(n)\boldsymbol{s}^H(n)\right\}\mathbf{A}^H\mathbf{W}\,.\end{aligned} \tag{10}$$

Note that, the beamspace manifold $\mathbf{W}^H\mathbf{A}$ is used for UCAs to calculate the BSCM in Eq. (10). With a large sample size, the first two terms of Eq. (10) are dominant, whereas the last two terms can be ignored compared to the first two terms. As a result, $\hat{R}_y$ in Eq. (10) is equal to R_y in Eq. (8). However,

if the sample size is small, this deviation deviates from R_y as the last two terms of Eq. (10) cannot be neglected and, obviously, DOAE performance will be reduced.

To eliminate the residual errors of the BSCM, i.e., the third and fourth components in Eq. (10), new method is proposed below to improve DOAE performance.

The proposed technique starts by transforming the observed measurements $\mathbf{X}$ in Eq. (1) into the beamspace measurements $\mathbf{Y}$ in Eq. (7) by the BT. Then, initial DOAs $\{\varphi'_1, \varphi'_2, \ldots, \varphi'_K\}$ are acquired through the UCARM method.

To achieve the corrected BSCM, we need to calculate the residual errors. The fourth component is the conjugated transpose and here we only derive the third component. A new beamspace manifold $\mathbf{W}^H\hat{\mathbf{A}}$ for UCAs is obtained based on initial DOAs. Then the estimated beamspace signal is expressed by the least squares method as:

$$s(n) = \left(\hat{\mathbf{A}}^H\mathbf{W}\mathbf{W}^H\hat{\mathbf{A}}\right)^{-1}\hat{\mathbf{A}}^H\mathbf{W}\boldsymbol{y}(n)\,. \tag{11}$$

Then, the third component of Eq. (10) is:

$$\begin{aligned} C_B &= \mathbf{W}^H\hat{\mathbf{A}}\left\{\frac{1}{N}\sum_{n=1}^{N}\hat{\boldsymbol{s}}(n)\hat{\boldsymbol{n}}_1^H(n)\right\} \\ &= \mathbf{W}^H\hat{\mathbf{A}}\frac{1}{N}\sum_{n=1}^{N}(\hat{\mathbf{A}}^H\mathbf{W}\mathbf{W}^H\hat{\mathbf{A}})^{-1}\hat{\mathbf{A}}^H\mathbf{W}\boldsymbol{y}(n) \\ &\quad \left\{\boldsymbol{y}^H(n) - \boldsymbol{y}^H(n)\mathbf{W}^H\hat{\mathbf{A}}\left(\hat{\mathbf{A}}^H\mathbf{W}\mathbf{W}^H\hat{\mathbf{A}}\right)^{-1}\hat{\mathbf{A}}^H\mathbf{W}\right\} \\ &= \hat{\mathbf{Q}}_B\left\{\frac{1}{N}\sum_{n=1}^{N}\boldsymbol{y}(n)\boldsymbol{y}^H(n)(\mathbf{I}-\hat{\mathbf{Q}}_B)\right\} \\ &= \hat{\mathbf{Q}}_B\hat{\mathbf{R}}_B(\mathbf{I}-\hat{\mathbf{Q}}_B) \end{aligned} \tag{12}$$

where subscript $(\cdot)_B$ denotes beamspace and:

$$\hat{\mathbf{Q}}_B = \mathbf{W}^H\hat{\mathbf{A}}\left(\hat{\mathbf{A}}^H\mathbf{W}\mathbf{W}^H\hat{\mathbf{A}}\right)^{-1}\hat{\mathbf{A}}^H\mathbf{W}\,.$$

The modified covariance matrix is as follows:

$$\hat{\mathbf{R}}'_y = \hat{\mathbf{R}}_y - \mu\left(C_B + C_B^H\right), \quad \mu \in [0,1]\,. \tag{13}$$

Consider Eqs. (8) and (10), μ is equal to one. Nevertheless, for the UCARM, a small residual systematic error caused by the BT is left over. Thus, the last two terms of Eq. (10) cannot be exactly estimated. In practice, μ is varied within the $0\ldots1$ interval to control the magnitude of the residual compensation term in Eq. (13). Since residual components are estimation-dependent and cannot be perfectly reconstructed, μ acts as a regularization factor that balances residual suppression and covariance stability. To achieve the corresponding DOAs, the RM will be utilized again per each μ.

To choose μ, which corresponds to the best azimuth angle estimates, the covariance matrix $\mathbf{R}_x = E\{\boldsymbol{x}(n)\,\boldsymbol{x}_H(n)\}$ is developed. Then, the EVD of the covariance matrix $\mathbf{R}_x$ is performed and $\mathbf{E}_{xn}$ is its element space noise subspace. We choose the DOAs $\{\varphi''_1, \varphi''_2, \ldots, \varphi''_K\}$ corresponding to the value of μ minimizing as the new DOAs:

$$P_{\mathrm{DOA}}(\mu) = P_M(\varphi''_1) + \ldots + P_M(\varphi''_K)\,, \tag{14}$$

where

$$P_M(\varphi''_i) = a^H(\varphi''_i)\,E_{xn}\,E_{xn}^H\,a(\varphi''_i) \tag{15}$$

and $(\cdot)''$ indicates the estimated parameters from the modified BSCM.

Considering the newly estimated DOAs, the beamspace sample covariance matrix (BSCM) can be recomputed using Eqs. (10), (12), and (13). Subsequently, the DOA estimation (DOAE) procedure is reapplied using the root-MUSIC (RM) technique. This process can be iteratively repeated to refine the DOAE results toward an optimal solution. Since the correction term in Eq. (13) is designed from a projection operator in the beamspace domain, the modified covariance matrix remains Hermitian and its dominant subspace structure is preserved across iterations. Although a higher number of iterations generally yields greater estimation accuracy, it also leads to increased computational complexity. It is important to note that the BSCM is modified in the beamspace domain specifically for the UCA configuration, rather than altering the element-space covariance matrix. Furthermore, since the residual components in the BSCM depend on the initial DOA estimates, they can only be eliminated after the first iteration and not beforehand. The complete workflow of the proposed UCARM-based algorithm can be summarized in the following sequential steps.

1) Initial DOAE using the UCARM.
2) Calculate the modified BSCM by Eqs. (10), (12), and (13). For each μ, use the UCARM again to obtain its corresponding DOAs. Choose the new DOAs based on Eq. (14).
3) Repeat step 2 to obtain the optimal DOAs.

The central idea of the proposed method is to iteratively refine the BSCM by removing residual error components. This iterative correction leads to enhanced DOAE accuracy compared to conventional approaches. The proposed UCARM algorithm demonstrates superior performance, particularly in scenarios involving correlated signals. Furthermore, the proposed technique is applicable to RARE-based methods combined with UCAs for 2D DOA estimation, especially under limited snapshot conditions [28], [29].

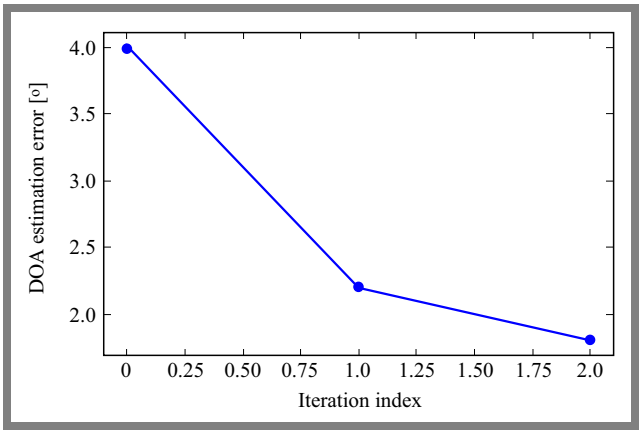

Fig. 1. DOA estimation error versus iteration number for the proposed BSCM refinement step.

Since the proposed refinement operates at the covariance level without altering the array manifold structure, it can be incorporated into 2D beamspace-based subspace frameworks without modifying their fundamental formulation. Although multiple iterations can be performed, empirical results indicate that one iteration provides more than 90% of the achievable improvement while keeping computational complexity low. Therefore, all simulations are conducted using a single iteration.

The convergence behavior of the refinement mechanism is illustrated in Fig. 1. As observed, the first iteration contributes more than 90% of the overall improvement, whereas additional iterations yield only marginal gains. This confirms that a single iteration is sufficient to ensure both accuracy and efficiency.

4. Performance Analysis

4.1. Error Analysis

The estimation error in DOAE is inherently linked to the accuracy of the BSCM. In this subsection, we focus on the error characteristics in the context of the UCARM algorithm. However, the insights and results presented here are not restricted to UCARM alone and can be extended to other methods that build on it.

The following derivations follow the classical subspace perturbation and polynomial sensitivity analysis framework established in [30]–[33] and are included here for completeness, in order to clarify the impact of covariance estimation errors. Similarly to Eq. (9), the sample rooting polynomial corresponding to UCARM is defined as:

$$\tilde{f}(\varphi) = \boldsymbol{a}_e^H(\varphi)\,\mathbf{F}^H(\theta)\,\hat{\mathbf{E}}_n\hat{\mathbf{E}}_n^H\,\mathbf{F}(\theta)\,\boldsymbol{a}_e(\varphi)\,. \tag{16}$$

In the following, the analysis is conducted how the BSCM affects the error is conducted. Based on the standard perturbation analysis in [30]–[33], it can be expressed as:

$$0 = \tilde{f}'(\hat{\varphi}_i) \approx \tilde{f}'(\varphi_i) + \tilde{f}''(\varphi_i)(\hat{\varphi}_i - \varphi_i)\,, \tag{17}$$

where $\tilde{f}'(\hat{\varphi}_i)$ is the first derivation and $\tilde{f}''(\varphi_i)$ is the second derivation of the sample polynomial. $\hat{\varphi}_i$ is the estimated azimuth angle and φ_i is the true azimuth angle of the i-th signal.

From Eq. (17), the error between the estimated and true azimuth angles is expressed as:

$$\hat{\varphi}_i - \varphi_i = -\frac{\tilde{f}'(\varphi_i)}{\tilde{f}''(\varphi_i)}\,, \tag{18}$$

where $\tilde{f}'(\varphi_i) = \partial\widetilde{f}(\varphi)/\partial\varphi|_{\varphi=\varphi_i}$.

To calculate the above mentioned two sample polynomials (first and second), we define the first derivation of $a_e(\varphi)$ as:

$$\boldsymbol{v}(\varphi) = -\frac{\partial a_e(\varphi)}{\partial\varphi}\,. \tag{19}$$

Then, the first derivation of the sample polynomial $\tilde{f}'(\hat{\varphi}_i)$ can be determined as:

$$\begin{aligned}\tilde{f}'(\varphi_i) &= \frac{\partial\tilde{f}(\varphi)}{\partial\varphi}\\ &= \frac{\partial\{\boldsymbol{a}_e^H(\varphi)F^H(\theta)\hat{\mathbf{E}}_n\hat{\mathbf{E}}_n^H F(\theta)\boldsymbol{a}_e(\varphi)\}}{\partial\varphi}\\ &= 2\,\mathrm{Re}\left[v^H(\varphi)\mathbf{F}^H(\theta)\hat{\mathbf{E}}_n\hat{\mathbf{E}}_n^H\mathbf{F}(\theta)\boldsymbol{a}_e(\varphi)\right]\end{aligned}\,. \tag{20}$$

$\mathrm{Re}\{.\}$ is considered as the real part of operator.

It can be approximated in this form since the second derivative term in Eq. (17) is multiplied by the estimation error, which is assumed to be sufficiently small under the first-order perturbation assumption [31]. Therefore, the second derivation of the sample polynomial is as follows:

$$\begin{aligned}\tilde{f}''(\varphi_i) \approx f''(\varphi_i) &= \frac{\partial f'(\varphi)}{\partial\varphi}\\ &= 2\,\mathrm{Re}\left\{\boldsymbol{v}^H(\varphi)\mathbf{F}^H(\theta)\hat{\mathbf{E}}_n\hat{\mathbf{E}}_n^H\mathbf{F}(\theta)\boldsymbol{v}(\varphi_i)\right\}\end{aligned}\,. \tag{21}$$

By considering Eqs. (19), (20) and (21), the error is given by:

$$(\hat{\varphi}_i - \varphi_i) = \frac{-\,\mathrm{Re}\left\{\boldsymbol{v}^H(\varphi_i)\mathbf{F}^H(\theta_i)\hat{\mathbf{E}}_n\hat{\mathbf{E}}_n^H\mathbf{F}(\theta_i)\boldsymbol{a}_e(\varphi_i)\right\}}{\boldsymbol{v}^H(\varphi_i)\mathbf{F}^H(\theta_i)\hat{\mathbf{E}}_n\hat{\mathbf{E}}_n^H\mathbf{F}(\theta_i)\boldsymbol{v}(\varphi_i)}\,. \tag{22}$$

Equation (22) indicates that the estimation error is governed by the mismatch between the true noise subspace $\mathbf{E}_n$ and its sample-based estimate, which is directly influenced by the accuracy of the BSCM.

Since the true noise subspace remains identical for both conventional and proposed approaches, the performance difference arises solely from the quality of the sample noise subspace estimate $\hat{\mathbf{E}}_n$ which, in turn, depends on the refined BSCM.

Unlike the non-recursive refinement scheme proposed in [1], which applies a single-pass modification of the BSCM, the method described in this paper iteratively updates the covariance matrix to enhance robustness against noise and snapshot limitations.

4.2. Beamspace Leakage

Leakage is related to the performance deterioration in cases with small sample size. It is caused by incomplete orthogonality between beamspace signals and noise subspaces from the BSCM. After performing the EVD of the beamspace sample covariance matrix $\hat{\mathbf{R}}_y$, we arrange the beamspace eigenvectors $\{\boldsymbol{e}_1,\ldots,\boldsymbol{e}_K,\ldots,\boldsymbol{e}_{2M+1}\}$ in a descending order.

Let $\hat{\mathbf{E}}_s = \{\hat{\boldsymbol{e}}_1,\hat{\boldsymbol{e}}_2,\ldots,\hat{\boldsymbol{e}}_K\}$ be the beamspace signal subspace and $\hat{\mathbf{E}}_n = \{\hat{\boldsymbol{e}}_{K+1},\hat{\boldsymbol{e}}_{K+2},\ldots,\hat{\boldsymbol{e}}_{2M+1},\}$ be the beamspace noise subspace. We define that the beamspace leakage after BT for UCA is the average value of beamspace sample signal eigenvectors projecting onto $\mathbf{E}_n\,\mathbf{E}_n^H$ as [27]:

$$\rho_B = \frac{1}{K}\sum_{k=1}^{K}\left\|\mathbf{E}_n\,\mathbf{E}_n^H\hat{\boldsymbol{e}}_k\right\|\,. \tag{23}$$

Ideally, $\hat{\mathbf{E}}_s$ and $\hat{\mathbf{E}}_n$ are orthogonal. Therefore, the average value of beamspace signal eigenvectors $\{\boldsymbol{e}_1,\ldots,\boldsymbol{e}_K\}$ projecting onto $\mathbf{E}_n\,\mathbf{E}_n^H$ is zero. Nevertheless, the beamspace leakage is

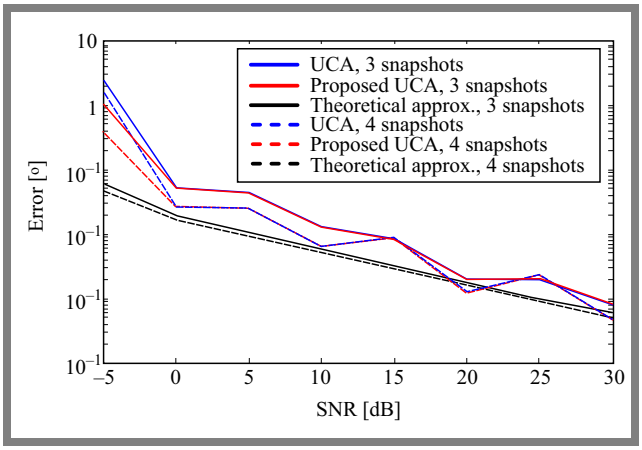

Fig. 2. Estimation error of DOA versus SNR for a single-source scenario ($\varphi = 50°$).

non-zero when the number of snapshots is small, because $\hat{\mathbf{E}}_s$ is not fully orthogonal to $\hat{\mathbf{E}}_n$. The beamspace leakage of the conventional algorithm can be expressed as [27]:

$$\rho_1 = \frac{1}{K}\sum_{k=1}^{K} \left\| \mathbf{E}_n \, \mathbf{E}_n^H \hat{\boldsymbol{e}}_k \right\| \cdot \frac{1}{K} \operatorname{Tr}\left((\mathbf{S})^{\dagger} \Delta \mathbf{R}_y' \mathbf{E}_n \, \mathbf{E}_n^H \Delta \mathbf{R}_y (\mathbf{S})^{\dagger} \right) , \tag{24}$$

where

$$\begin{aligned} (\mathbf{S})^{\dagger} &= \mathbf{S}(\mathbf{S}^H \mathbf{S})^{-1}, \\ \mathbf{S} &= \mathbf{W}^H \mathbf{A} \mathbf{R}_s \, \mathbf{A}^H \mathbf{W}, \\ \Delta \mathbf{R}_y' &= \hat{\mathbf{R}}_y - \mathbf{R}_y. \end{aligned}$$

For the proposed algorithm with one repetition (Step 3 in Section 3), the beamspace leakage is given as:

$$\begin{aligned} \rho_2 &= \frac{1}{K}\sum_{k=1}^{K} \left\| \mathbf{E}_n \, \mathbf{E}_n^H \hat{\boldsymbol{e}}_k'' \right\| \\ &= \frac{1}{K} \operatorname{Tr}\left((\mathbf{S})^{\dagger} \Delta \mathbf{R}_y'' \, \mathbf{E}_n \, \mathbf{E}_n^H \Delta \mathbf{R}_y'' (\mathbf{S})^{\dagger} \right) \end{aligned} , \tag{25}$$

where

$$\Delta \mathbf{R}'' = \hat{\mathbf{R}}_y - \mathbf{R}_y - \gamma \left(\mathbf{C}_B + \mathbf{C}_B^H \right) .$$

4.3. Computational Complexity

The computational complexity of the conventional UCARM algorithm is dominated by the eigen-decomposition and polynomial rooting steps, resulting in an overall complexity of $\mathcal{O}(P^3 + N \cdot K \cdot P^2)$. The proposed refinement technique introduces one additional update of the BSCM with computational cost $\mathcal{O}(P^2 K + P^3)$ per iteration. Since only a single iteration is applied in practice, the total complexity remains comparable to that of conventional UCARM, while offering significantly improved estimation accuracy. The additional computational overhead is therefore bounded and does not alter the overall cubic-order complexity of the underlying subspace-based framework.

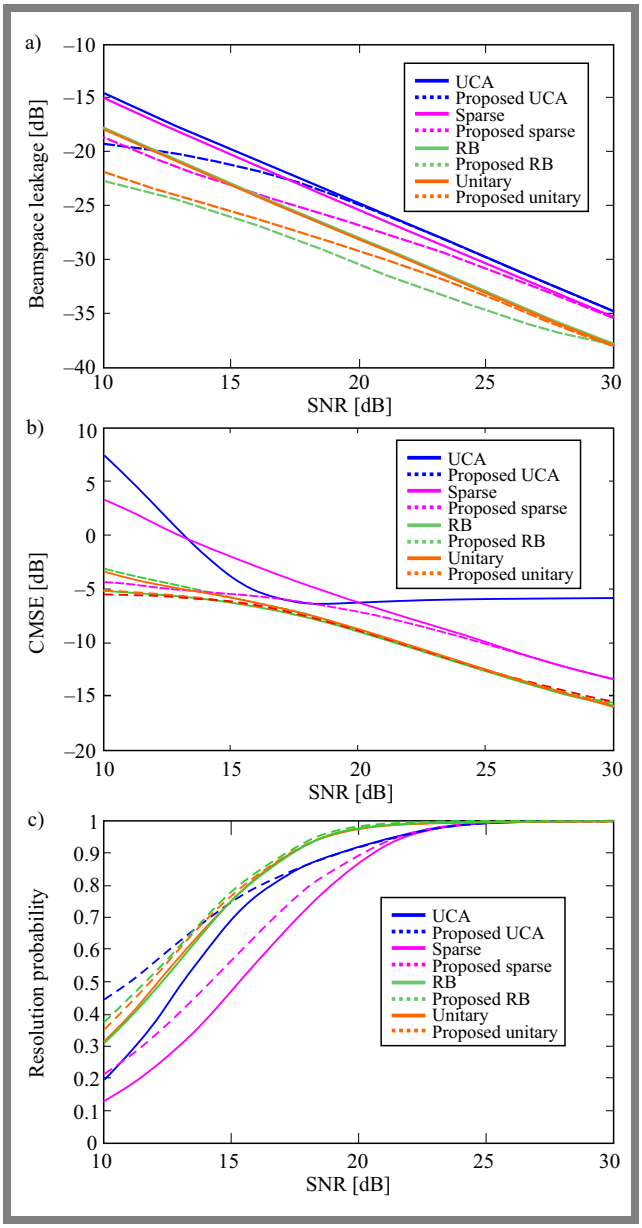

Fig. 3. Performance for uncorrelated signals versus SNR: a) beamspace leakage, b) CMSE, and c) resolution probability.

5. Simulation Results

In the simulation setup, a UCA consisting of 17 elements is used. The radius of the matrix is set to a constant value (λ/2), and the tuning parameter α varies from 0 to 1, in increments of 0.1. All signals are assumed to arrive at a fixed elevation angle of 80°, and a single iteration of step 3 (from the proposed algorithm) is considered in the simulations.

To further validate the effectiveness of the proposed technique, three additional proposed variants are also implemented for comparison: UCARB RM, sparse UCARM, and unitary UCARM. For clarity, the following abbreviations are used: UCARM [11] as UCA, sparse UCARM [23] as sparse, UCARBRM [11] as RB, and unitary UCARM [19] as unitary. The sparse UCARM configuration utilizes nine antenna elements.

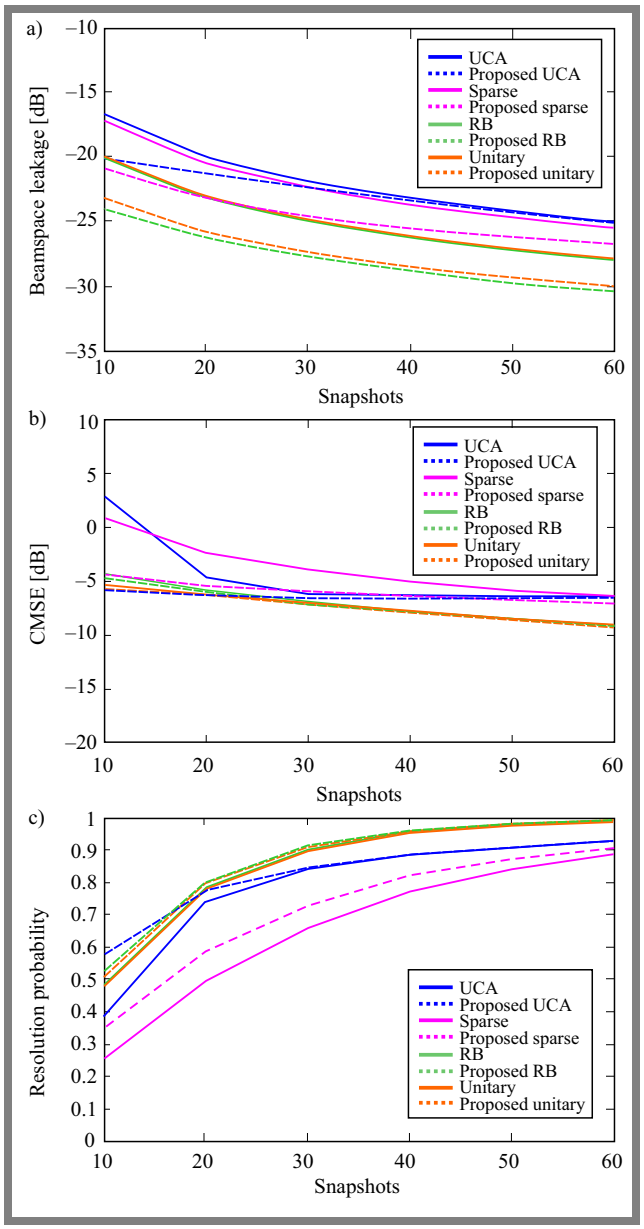

Fig. 4. Performance for uncorrelated signals versus snapshots: a) beamspace leakage, b) CMSE, and c) resolution probability.

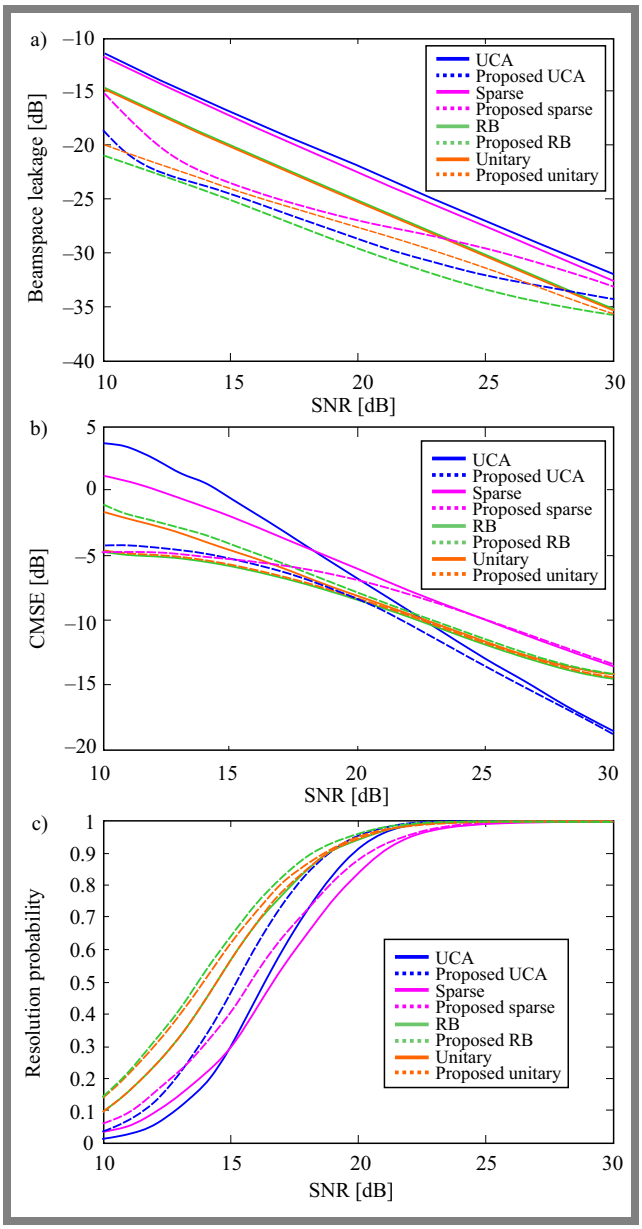

Fig. 5. Performance for correlated signals versus SNR: a) beamspace leakage, b) CMSE, and c) resolution probability.

5.1. Error Performance Analysis

In this scenario, a single-source signal impinging from the azimuth angle of $\varphi = 50°$ is considered. The error performance of the proposed algorithm is evaluated using 1 000 Monte Carlo simulations under two snapshot conditions: 3 and 4 snapshots. As illustrated in Fig. 2, the relationship between estimation error and SNR shows that the proposed UCA-based algorithm consistently outperforms its conventional counterpart in both snapshot cases, particularly in low SNR regimes. This improved performance is primarily attributed to the elimination of residual components in the BSCM, which effectively mitigates interference between the signal and noise subspaces in the beamspace domain.

5.2. Performance for Uncorrelated Signals

To evaluate the performance of the proposed algorithms in terms of beamspace leakage, conditional mean squared error (CMSE), and resolution probability simulations are conducted using equi-powered uncorrelated signals. CMSE is defined as the mean squared error under the condition that all sources are detected correctly. The resolution probability refers to the probability that the difference between the estimated and true DOAs is less than one degree for all signal directions. The evaluations are based on 10 000 Monte Carlo trials.

In the simulation analysis, two uncorrelated signals impinge on the array from azimuth angles of 50° and 56°, with the number of snapshots fixed at 15. The results for beamspace leakage, CMSE, and resolution probability versus SNR are shown in Fig. 3.

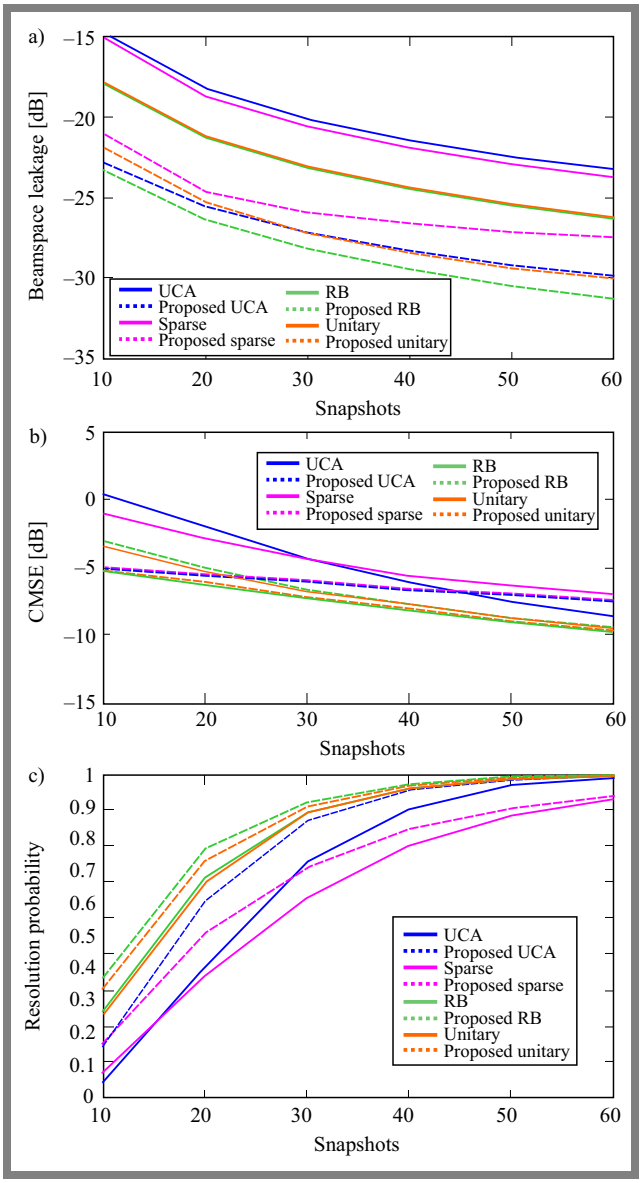

Fig. 6. Performance for correlated signals versus snapshots: a) beamspace leakage, b) CMSE, and c) resolution probability.

As depicted in Fig. 3a, all proposed algorithms demonstrate significantly lower beamspace leakage than their respective conventional counterparts. Beamspace leakage is reduced by approximately 5 dB when the SNR is below 13 dB. The proposed RB algorithm achieves the lowest leakage due to the use of forward/backward averaging.

Figure 3b illustrates that all proposed algorithms achieve significant improvements in CMSE over conventional ones, with the proposed UCA showing the most significant enhancement. Similarly, Fig. 3c shows that the proposed methods outperform their counterparts in terms of resolution probability. At SNR values below 15 dB, the proposed UCA provides the best resolution performance, while at higher SNRs, the proposed RB achieves superior accuracy.

Figure 4 shows the performance on beamspace leakage, CMSE and resolution probability versus snapshots with SNR=14 dB. The results versus snapshots are similar to those versus SNR.

5.3. Performance for Correlated Signals

Assume that two correlated signals with the correlation coefficient of 0.8 impinge on the UCA from $\varphi_1 = 50^\circ$ and $\varphi_2 = 60^\circ$. The number of snapshots is 15. Figure 5 illustrates the performance of the algorithms in terms of beamspace leakage, CMSE, and resolution probability as functions of SNR.

As observed in Fig. 5a, all proposed methods outperform their conventional counterparts in reducing beamspace leakage. The proposed UCA algorithm achieves the most significant reduction exceeding 6 dB, when the SNR is 10 dB. Furthermore, Fig. 5b confirms that the proposed method effectively lowers CMSE, primarily due to the improved formulation of the BSCM, which is consistent with the trend observed earlier in Fig. 3b. Moreover, as shown in Fig. 5b, the proposed RB algorithm delivers outstanding performance, primarily due to its real-valued processing scheme. In Fig. 5c, all four proposed algorithms demonstrate significant improvements in resolution probability compared to their conventional counterparts.

Figure 6 illustrates the impact of varying the number of snapshots on the performance of two correlated signals at a fixed SNR of 15 dB. As expected, the proposed algorithms consistently outperform their traditional versions across all metrics.

From Figs. 3 to 6, it is evident that all proposed algorithms consistently outperform their conventional counterparts in terms of SNR and snapshot variations, both for uncorrelated or correlated signal scenarios. These results confirm that the proposed approach can be extended to a variety of BT-based Root-MUSIC (RM) frameworks, including UCA-RARE methods for 2D DOAE applications. Therefore, the BSCM refinement technique introduced in this work offers broad applicability for enhancing the accuracy of DOA estimation.

Among the proposed methods, the RB and unitary variants show the best performance for uncorrelated signals, while the UCA and Sparse variants perform comparatively worse. The sparse algorithm shows the weakest results, which can be attributed to the reduced number of its antenna elements. On the other hand, Figs. 5 and 6 clearly indicate that the proposed RB method delivers superior efficiency in scenarios involving correlated signals.

Figure 7 shows the probability of resolution as a function of the correlation coefficient with a fixed SNR of 15 dB. As observed, all proposed algorithms significantly outperform their conventional counterparts. Among them, the proposed unitary algorithm exhibits the best overall performance.

In Fig. 8, the performance of the proposed RB algorithm is examined with respect to resolution probability versus angular separation, considering both correlated and uncorrelated signal scenarios.

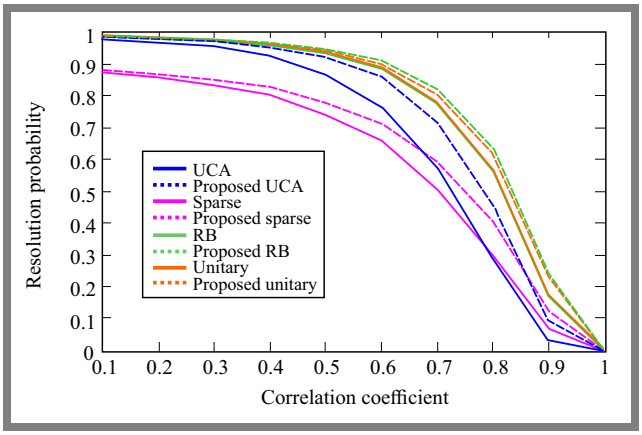

Fig. 7. Resolution probability versus correlation coefficient.

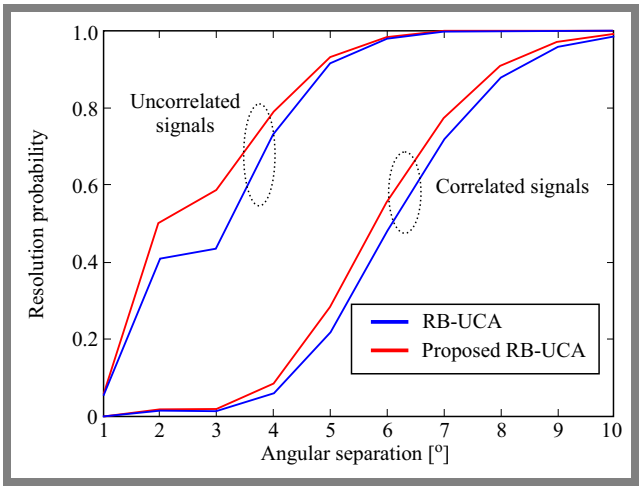

Fig. 8. Probability of resolution versus angular separation for correlated ($\rho = 0.7$) and uncorrelated cases.

The correlation coefficient for the correlated case is set to 0.7, and the SNR is fixed at 20 dB. The results of Fig. 8 confirm that the proposed RB algorithm consistently outperforms the conventional RB method, regardless of the presence or absence of signal correlation.

6. Conclusions

In this paper, an iterative enhancement technique was proposed to improve the accuracy of direction-of-arrival estimation (DOAE) for uniform circular arrays (UCA), particularly under limited snapshot conditions. The method is based on repeatedly refining the beamspace sample covariance matrix (BSCM) by eliminating residual components that degrade performance, especially at low signal-to-noise ratios (SNRs) or when few observations are available.

The technique integrates an initial estimation using the root-MUSIC algorithm in the beamspace domain, followed by iterative correction of the BSCM, using least-squares reconstruction and controlled adjustment of a tunable regularization parameter. This approach results in improved accuracy of the estimated directions through better modeling of the signal and noise subspaces.

Detailed simulation results demonstrate that the proposed method significantly outperforms conventional UCARM, sparse UCARM, UCARBRM, and unitary UCARM methods in terms of estimation error, beamspace leakage, conditional mean square error (CMSE) and resolution probability for both uncorrelated and correlated signal scenarios. The proposed technique is also applicable to 2D DOAE frameworks such as RARE-based algorithms, while preserving the underlying beamspace covariance structure.

Overall, the proposed BSCM refinement strategy offers a promising solution for high-accuracy DOAE in UCA configurations with limited data and can be readily integrated into a wide range of beamspace-based subspace estimation methods. Compared with previous single-step refinement methods, such as [1], the proposed iterative strategy provides more consistent performance across different SNRs and snapshot sizes, while maintaining comparable computational complexity.

References

[1] G. Jiang, X. Mao, and Y. Liu, “Reducing Errors for Root-MUSIC-based Methods in Uniform Circular Arrays”, *IET Signal Processing*, vol. 11, pp. 1055–1062, 2017 (https://doi.org/10.1049/iet-spr.2016.0576).

[2] Y. Zhang, Y. Wang, and Y. Zhang, “DOA Estimation Based on Deep Learning with Sparse Uniform Circular Array”, *IET Radar, Sonar & Navigation*, vol. 15, pp. 1171–1179, 2021 (https://doi.org/10.1049/rsn2.12168).

[3] A. Aydoğan and B.S. Yarman, “Enhanced Beamspace Processing for Direction-of-arrival Estimation Using Uniform Circular Arrays”, *Turkish Journal of Electrical Engineering & Computer Sciences*, vol. 28, pp. 974–987, 2020 (https://doi.org/10.3906/elk-1903-125).

[4] H. Li, J. Wang, and X. Chen, “Robust Direction-of-arrival Estimation Approach Using Beamspace Transform and Array Imperfections Compensation”, *IET Radar, Sonar & Navigation*, vol. 16, pp. 1605–1619, 2022 (https://doi.org/10.1049/rsn2.12282).

[5] M. Sharifi and P. Rezaei, “Conformal Antenna Array Radiation Pattern Synthesis by Tilt Correction to Improve Direction-of-arrival Estimation Accuracy”, *Electromagnetics*, vol. 40, pp. 262–275, 2020 (https://doi.org/10.1080/02726343.2020.1757138).

[6] Y. Wang, W. Tan, Z. Deng, and G. Li, “Low-complexity Sparse Beamspace DOA Estimation via Single Measurement Vectors for Uniform Circular Array”, *Turkish Journal of Electrical Engineering & Computer Sciences*, vol. 29, pp. 1973–1987, 2021 (https://doi.org/10.3906/elk-2010-109).

[7] M. Sharifi and P. Rezaei, “Near Optimal Conformal Antenna Array Structure for Direction-of-arrival Estimation”, *International Journal of RF and Microwave Computer-Aided Engineering*, vol. 29, art. no. e21978, 2019 (https://doi.org/10.1002/mmce.21978).

[8] T. Chen, L. Liu, and L. Guo, “Joint Carrier Frequency and DOA Estimation Using a Modified ULA Based MWC Discrete Compressed Sampling Receiver”, *IET Radar, Sonar & Navigation*, vol. 12, pp. 873–881, 2018 (https://doi.org/10.1049/iet-rsn.2017.0505).

[9] S. Shi, Y. Xu, and Z. Liu, “Block Sparse Representation Approach to 2D DOA and Polarization Estimation of Wideband Signals Using a Sparse Vector Antenna Array”, IET Radar, Sonar & Navigation, vol. 14, pp. 1929–1939, 2020 (https://doi.org/10.1049/iet-rsn.2020.0152).

[10] A. Akgül and B.S. Yarman, “Robust Beamspace DOA Estimation for Uniform Circular Arrays Using Modified Correlation Processing”, *Turkish Journal of Electrical Engineering & Computer Sciences*, vol. 27, pp. 3006–3018, 2019 (https://doi.org/10.3906/elk-1811-30).

[11] C.P. Mathews and M.D. Zoltowski, "Eigenstructure Techniques for 2-D Angle Estimation with Uniform Circular Arrays", *IEEE Transactions on Signal Processing*, vol. 42, pp. 2395–2407, 1994 (https://doi.org/10.1109/78.317861).

[12] H. Li, J. Wang, and X. Chen, "Robust Direction-of-arrival Estimation Approach Using Beamspace Transform and Array Imperfections Compensation", *Turkish Journal of Electrical Engineering & Computer Sciences*, vol. 30, pp. 1605–1619, 2022 (https://doi.org/10.3906/elk-2111-127).

[13] A. Liu *et al.*, "Augmented Subspace MUSIC Method for DOA Estimation Using Acoustic Vector Sensor Array", *IET Radar, Sonar & Navigation*, vol. 13, pp. 969–975, 2019 (https://doi.org/10.1049/iet-rsn.2018.5440).

[14] M. Sharifi, P. Rezaei, and S. Mohammadi, "DOA Estimation Accuracy Improvement by Solving the Rank Reduction Algorithm Ambiguous Parameters Through Synthesizing the Volume Antenna Beam Pattern", *International Journal of RF and Microwave Computer-Aided Engineering*, vol. 32, art. no. e23465, 2022 (https://doi.org/10.1002/mmce.23465).

[15] K.M. Reddy and V.U. Reddy, "Analysis of Spatial Smoothing with Uniform Circular Arrays", *IEEE Transactions on Signal Processing*, vol. 47, pp. 1726–1730, 1999 (https://doi.org/10.1109/78.765637).

[16] N.P. Waweru, D.B.O. Konditi, and P.K. Langat, "Performance Analysis of MUSIC, Root-MUSIC and ESPRIT DOA Estimation Algorithm", *International Journal of Electronics and Communication Engineering*, vol. 8, pp. 209–216, 2014.

[17] M. Sharifi, M. Boozari, M.G. Alijani, and M.H. Neshati, "Development a New Algorithm to Reduce SLL of an Equally Spaced Linear Array", *2018 Iranian Conference on Electrical Engineering (ICEE)*, Mashhad, Iran, 2018 (https://doi.org/10.1109/ICEE.2018.8472591).

[18] C. Kassis, J. Picheral, and C. Mokbel, "Advantages of Nonuniform Arrays Using Root-MUSIC", *Signal Processing*, vol. 90, pp. 689–695, 2010 (https://doi.org/10.1016/j.sigpro.2009.08.006).

[19] F. Belloni and V. Koivunen, "Unitary Root-MUSIC Technique for Uniform Circular Array", *2003 IEEE International Symposium on Signal Processing and Information Technology (ISSPIT)*, Darmstadt, Germany, 2003 (https://doi.org/10.1109/ISSPIT.2003.1341160).

[20] M. Pesavento, A.B. Gershman, and M. Haardt, "Unitary Root-MUSIC with a Real-valued Eigendecomposition: A Theoretical and Experimental Performance Study", *IEEE Transactions on Signal Processing*, vol. 48, pp. 1306–1314, 2000 (https://doi.org/10.1109/78.839978).

[21] C. Qian, L. Huang, and H.C. So, "Improved Unitary Root-MUSIC for DOA Estimation Based on Pseudo-noise Resampling", *IEEE Signal Processing Letters*, vol. 21, pp. 140–144, 2013 (https://doi.org/10.1109/LSP.2013.2293949).

[22] G.J. Jiang, X.P. Mao, and Y.T. Liu, "Coprime Sparse Circular Array with Little Angular Dependence and Reduced Mutual Coupling", *AEU – International Journal of Electronics and Communications*, vol. 117, art. no. 153051, 2020 (https://doi.org/10.1016/j.aeue.2020.153051).

[23] R. Goossens, H. Rogier, and S. Werbrouck, "UCA Root-MUSIC with Sparse Uniform Circular Arrays", *IEEE Transactions on Signal Processing*, vol. 56, pp. 4095–4099, 2008 (https://doi.org/10.1109/TSP.2008.921764).

[24] F. Belloni and V. Koivunen, "Beamspace Transform for UCA: Error Analysis and Bias Reduction", *IEEE Transactions on Signal Processing*, vol. 54, pp. 3078–3089, 2006 (https://doi.org/10.1109/TSP.2006.875395).

[25] V. Vasylyshyn, "Removing the Outliers in Root-MUSIC via Pseudo-noise Resampling and Conventional Beamformer", *Signal Processing*, vol. 93, pp. 3423–3429, 2013 (https://doi.org/10.1016/j.sigpro.2013.04.012).

[26] J. Cao *et al.*, "Broadband Signal DOA Estimation Based on Two-sided Correlation Transformation Using Array Manifold Interpolation", *IET Radar, Sonar & Navigation*, vol. 19, art. no. e12669, 2025 (https://doi.org/10.1049/rsn2.12669).

[27] M. Shaghaghi and S.A. Vorobyov, "Subspace Leakage Analysis and Improved DOA Estimation with Small Sample Size", *IEEE Transactions on Signal Processing*, vol. 63, pp. 3251–3265, 2015 (https://doi.org/10.1109/TSP.2015.2422683).

[28] B.H. Wang, H.T. Hui, and M.S. Leong, "Decoupled 2D Direction of Arrival Estimation Using Compact Uniform Circular Arrays in the Presence of Elevation-dependent Mutual Coupling", *IEEE Transactions on Antennas and Propagation*, vol. 58, pp. 747–755, 2009 (https://doi.org/10.1109/TAP.2009.2039299).

[29] J. Dai *et al.*, "A Recursive RARE Algorithm for DOA Estimation with Unknown Mutual Coupling", *IEEE Antennas and Wireless Propagation Letters*, vol. 13, pp. 1593–1596, 2014 (https://doi.org/10.1109/LAWP.2014.2345564).

[30] P. Stoica and A. Nehorai, "Performance Study of Conditional and Unconditional Direction-of-arrival Estimation", *IEEE Transactions on Acoustics, Speech, and Signal Processing*, vol. 38, pp. 1783–1795, 1990 (https://doi.org/10.1109/29.60109).

[31] A.L. Swindlehurst and T. Kailath, "A Performance Analysis of Subspace-based Methods in the Presence of Model Errors. I. The MUSIC Algorithm", *IEEE Transactions on Signal Processing*, vol. 40, pp. 1758–1774, 1992 (https://doi.org/10.1109/78.143447).

[32] J. Xie, Z. He, H. Li, and J. Li, "2D DOA Estimation with Sparse Uniform Circular Arrays in the Presence of Mutual Coupling", *EURASIP Journal on Advances in Signal Processing*, vol. 2011, art. no. 80, 2011 (https://doi.org/10.1186/1687-6180-2011-80).

[33] L. Yang and Y. Zhang, "Performance Analysis of Root-MUSIC Algorithm for DOA Estimation Under Small Sample Size", *IET Radar, Sonar & Navigation*, vol. 1, pp. 91–98, 2007 (https://doi.org/10.1049/iet-rsn:20060014).

Mahdi Sharifi, Ph.D.
Department of Electrical and Computer Engineering
https://orcid.org/0000-0003-2675-8189
E-mail: m.sharifi@semnan.ac.ir
Semnan University, Semnan, Iran